Validated efficiency improvements by implementation of structures on the slipper surface of an axial piston pump

Svenja Horn, Roman Ivantysyn, Jürgen Weber

Institute of Mechatronic Engineering, TU Dresden, svenja.horn@tu-dresden.de, roman.ivantysyn@tu-dresden.de, juergen.weber@tu-dresden.de

Abstract.

New application areas such as compact drives and displacement control using variable electric motors require that hydrostatic machines exhibit good performance also at very low relative speeds without being damaged during critical mixed friction conditions. Low relative speeds result in a drop of the hydrodynamic pressure in the lubricating gaps and therefore to friction losses, wear and a higher probability of failures. The aim of this paper is to present a novel approach to reduce the viscous friction losses and wear during critical operating conditions, by increasing the hydrodynamic pressure build-up and modify the hydrostatics of the slippers of an axial piston pump. To achieve this goal structured surface profiles on the slipper surface are investigated, both in simulation and measurement. The measurement results and simulation validation are shown in this paper.

Keywords. Axial piston pump, slippers, surface structures, lubricating gap, numerical simulation, tribology**.**

1 INTRODUCTION

Electrification and compact drives are becoming popular due to environmental benefits and their ease of operation and plug-and-play. However, the pumps in these drives are exposed to very critical mixed friction conditions, especially at low speeds and high pressures. Low relative speeds result in a drop of the hydrodynamic pressure in the lubricating gaps and therefore to friction losses, wear and a higher probability of failures. Usually, material combinations of leaded bronze or brass and steel are used to ensure good run-in behavior and thus good dry-running performance under mixed friction. However, EU regulations require that lead-containing materials should no longer be used in the future. This makes it necessary to find other materials and structures that can withstand the tougher operating conditions despite the absence of lead containing metals. In order to avoid lead in the lubrication gaps, new designs must be investigated to reduce wear in the first place.

The research goal was to develop a novel approach to reduce the viscous friction losses and wear during critical operating conditions by increasing the hydrodynamic pressure build-up of the slippers of an axial piston pump. In order to achieve this objective, structured surface profiles are investigated to be adapted to the slipper surface, which is one of the three main lubricating interfaces, see Figure 1.1, and significantly contributes to the pumps powerlosses. In cooperation with the Fraunhofer IWU Chemnitz the manufacturing limitations for series production of the structured surface are analyzed for different materials. This paper presents the measurement results of the developed designs.

On the right side of Figure 1.1 the optimization problem of the lubrication interfaces is shown. A trade-off arises due to the conflicting requirements on the gap to allow good bearing properties while reducing leakage at the same time. The powerloss curve on the right of the figure depicts this correlation with a theoretical parallel gap height. Unfortunately, the optimum gap height changes with each operating condition, further increasing the complexity of the design process.

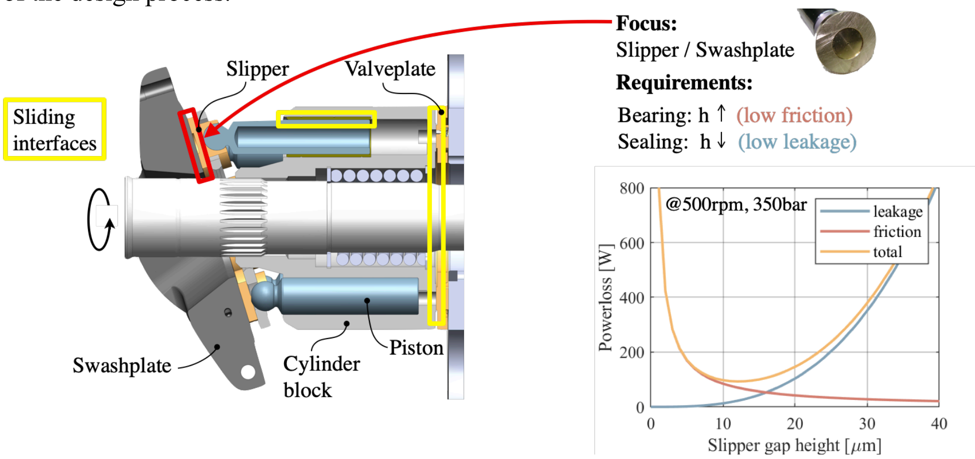

Figure 1.1. Sliding interfaces of the axial piston pump (left) and calculation of the powerlosses of a single slipper (right)

2 RESEARCH GOAL AND APPROACH

There are two main physical mechanisms that affect the gap height that occurs at a certain operating condition (OC), which apply to both the slipper/swash plate and valve plate/cylinder block interfaces. First the hydrostatic pressure that is directly correlating to the pressure in the piston and the area they act on. Second, the hydrodynamic pressure that is essentially resulting from the rotational speed. A pump designer needs to choose a certain speed range for his design, which defines the amount of hydrodynamics. The hydrostatics are adjusted to the hydrodynamics. However, this implies that for certain operating conditions (OCs) with low pressures and low speeds, insufficient hydrodynamic and hydrostatic forces are present to ensure an adequate fluid film to be formed. As shown in Figure 2.1, this can lead to mixed friction and wear. Using traditional approaches, such as increasing the pocket size or changing the orifice of the slipper, one can change the distribution of the powerlosses, either having a well performing slipper at low speeds and pressures or having optimal powerlosses at high speeds and high pressures, but typically not both. Surface structures open-up the possibility to perform well at all regimes.

Using simulation three designs were selected and manufactured. This paper shows the measurement results as well as the comparison to simulation results as validation.

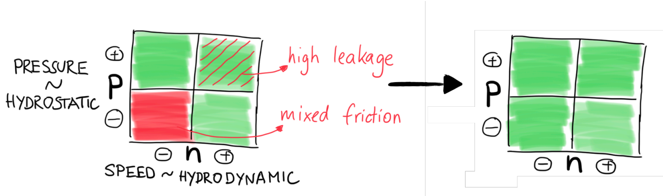

Figure 2.1. Research goal: Increase of load capacity especially at low speeds without worsening at high speeds and pressures

3 LITERATURE

In the past there have been quite a few researchers that investigated surface structures and modifications on hydrodynamic bearings, not that many have incorporated these also on surfaces used for hydrostatics. Due to space limitations the next section only covers the ones that built and tested these structures on hydrostatic bearings. One can distinguish the efforts in structural regimes. Micro, meso and macro structures. Micro structures usually have a depth to length ratio of 1:10 both being in the µm range. First efforts of these kinds were tested in the automotive industry to reduce friction between the piston and the bore of combustion engines. They can lead to friction reductions of up to 55% [1]. In hydraulic pumps this was tested by [2], [3]. Here various micro dimples were tested on many parts such as bearings, gear pumps, pistons and valve plates. It was shown that these micro holes were beneficial for purely hydrodynamic bearings such as the piston. However, for hydrostatic bearings they are contra-productive as they disturb the pressure field of the hydrostatics, which was not accounted for in the simulation models. In contrast, Baker used an earlier version of Caspar, a more sophisticated simulation tool that is also used for the simulations of this paper, to design waved like structures on a valve plate. Those were in the meso-region, meaning depth were in micrometer range but wave lengths in millimeter (1:1000). Baker developed a very promising design and demonstrated up to 10% decrease in powerlosses while also showing a tremendous reduction in wear [4]. These meso-structures turned out to be more successful with hydrostatic sealings as shown in simulation in the piston-cylinder interface by Ivantysynova, Lasaar, Ernst, and Wondergem [5]–[7]. The proposed step design in this paper could be mistaken with a step design patented by Ivantysyn in 1997 [8]. While this step height is similar in size, it serves a different purpose. Here the pocket diameter is self-adjusting with small gap heights, essentially increasing the pocket diameter when gap heights decrease to only a few µm. This step is in the opposite direction as the proposed step, removing material at the inner diameter instead of adding to it. Macro structures, meaning depth and length in millimeter range, have been found to be beneficial in hydrodynamic thrust bearings as demonstrated by some companies [9]. However, their use in hydraulics is not applicable due to their deep grooves and therefore total loss of hydrostatics.

4 OVERVIEW OF PREVIOUS SIMULATION RESULTS

4.1 Methodology

For the development of a wear free slipper that is well performing in low and also high speed regimes, an extensive simulation effort was expended (over 4400 simulations / 36,000 CPU hours) using the latest version of Caspar FSTI, which includes deformations due to pressure and temperature. First a competitive baseline with no structure was designed using computational design methods. The test pump was a Parker PV series (92cc) with a decreased slipper outer diameter to reflect the mean of five leading pump manufacturers to give these results a more general foundation. This baseline represents the very best possible single land design for this given piston size (21 mm diameter) and will serve as a reference. A single land design was chosen to accorporate the largest possible surface area, which is beneficial for low-speed applications. The optimization goals were minimization of overall powerloss due to leakage and friction and the minimization or total avoidance of material wear. The whole design process is illustrated in [10].

Using the same criteria but adding multiple forms of freedom in the surface topology different surface structures were designed and analyzed, the very best being a waved structure and a step structure. These three designs (flat reference, wave and step) were manufactured using state of the art series manufacturing methods such as turning or stamping and are shown in Figure 4.1. These slippers were tested in the same run-in pump and compared to each other.

4.2 Selected Operating Conditions (OCs)

In order to reduce simulation time while retaining a representative operational space, the number of investigated OCs were limited to a distinct selection. Table 4.1 shows the selected four OCs with different speeds n, pressure drops Δp and swashplate angles β, inducing crucial conditions in the operation of a pump. OC1 with low speed and low working pressure represents start-up or idle situation. During these conditions it is most likely that mixed friction and abrasion can occur due to insufficient hydrodynamic pressure built up. OC2 with low speed but high pressure is typical for load holding situations, a typical condition for high leakage losses, which need to be prevented. High speed and low pressure for OC3 result in high centrifugal forces that tend to tilt the slipper such that wear is to be feared. An additionally low swashplate angle induces lift off and high leakages, which needs to be prevented. OC4 with maximum power from high speed and high pressure is usually resulting in higher leakage values and often generates high thermal load, making it prone to temperature and pressure deformations, which need to be accounted for. OC4 also represents a very significant OC for the OEMs and their customers.

Table 4.1 Definition of operating conditions (OCs)

OC	n [rpm]	Δp [bar]	β [%]	represents
1	500	50	100	Idle
2	500	350	100	Low flow high load
3	1800	50	20	Prevent slipper lift-off
4	1800	350	100	Max. power

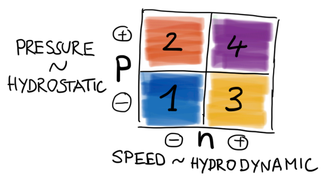

4.3 Final designs and comparison to reference design

Figure 4.1 shows pictures of the final manufactured designs, which were the outcome of the simulation optimization. On the left is the reference slipper with a balance of 99%. The balance factor is an indicator of the slipper's pocket size and is described along with the entire design process in more detail in [10], [11] and given in (1). It is calculated by dividing the hydrostatic force F_{fz}, that is estimated as logarithmic pressure drop over the sealing land, by the force of the piston on the slipper F_{SK}:

$$B = \frac{F_{fz}}{F_{SK}} \tag{1}$$

The wave slipper is shown in the centre of Figure 4.1. The structure is visible with the naked eye, but is mainly due to stepped surface topology, which was easier to manufacture and had no significant effect on the performance according to simulation studies. The balance of the wave slipper is at 102%, indicating that the pocket of the sealing land is larger than the reference. The pressure drop is influenced by the wave, otherwise the slipper would lift off and have an excessive amount of leakage at higher pressures. To the right side of Figure 4.1 is the step slipper. For this slipper the inner sealing land is 6 µm higher than the outer one. The step in between the two sealing lands can barely be seen, its only indicated by the 6 radial lines around the centre of the sealing land. Each line represents a 1 µm increase. The balance is even higher here at 105%, making this indicator purely a pocket size rather than a performance factor.

Figure 4.1. Final structured designs with optimized parameters and reference design

The optimization of the slippers was performed for the 4 OCs mentioned earlier in this chapter. The 4 OCs were weighted equally, therefore the optimization was the reduction of the sum of the powerlosses. Figure 4.2 shows the simulated performance gains from the two structured designs in comparison to the reference. In sum over all four OCs the wave design shows powerloss reductions by 9% and the step design by even 38%. The overall aim of the study, to improve low speed performance (OC1) without a significant efficiency decrease at higher speeds and pressures, has already been reached with the wave design. This is indicated by the plot on the right of Figure 4.2, which shows the individual powerlosses at each OC. An 85% reduction in powerlosses at low speed and low pressure (OC1) can be achieved by adding a waved surface to the slipper. The step design achieves a similar powerloss reduction of 88% for OC1, while performing better at the other OCs as well, which greatly surpasses the initial goal. Both, wave and step design achieve an improvement of over 10% of the total pump efficiency for OC1. A possible reason for the great performance of both the wave and the step design at low speeds and low pressures (OC1) is the increased hydrodynamics due to the surface structures. Further investigations for a better understanding of the underlying physics are in progress. A comparison of the designs with the same pocket size to show the isolated influence of the shaping itself has been shown in [10].

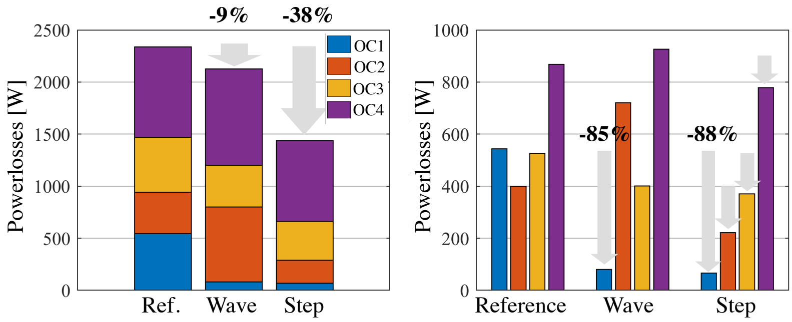

Figure 4.2. Comparison of powerlosses for the final designs and the reference in cumulation (left) and individually by operating condition (OC) (right)

5 EFFICIENCY MEASUREMENTS OF STRUCTURED SLIPPERS IN COMPARISON TO A FLAT REFERENCE SLIPPER

5.1 Steady state test rig and measurement procedure

The pump used in this study was a Parker PV 92cc series, which is an open circuit pump with a variable swash plate. The test rig used for these tests along with the used sensors is illustrated in Figure 5.1 and Table 5.1.

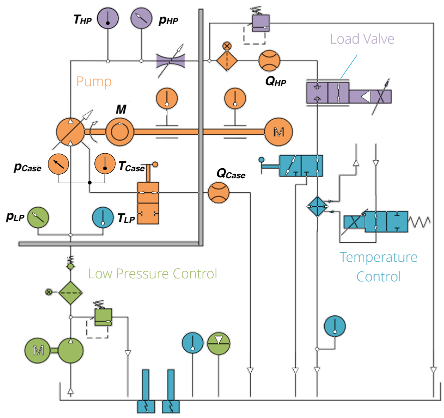

Figure 5.1. Test rig schematic

The next section shows the measurement results for various designs of the slippers. All measurements were performed in a stationary manner, meaning the conditions were held until temperature, flow and torque stabilized. When performing pump test rig measurements, it is obvious that the resulting leakage and torque reflect the entire pump, not just the slippers. Therefore, improvements can only be measured relative to each other, and it is necessary to have a solid baseline to which these design changes can be compared to. Pumps and their lubricating gaps typically go through a wear-in process, during which the efficiency also changes.

Table 5.1. Electronic sensors and accuracies

Para-meter	Sensor data		
	Sensor	***Type***	***Accuracy***
M	Torque meter	HBM T10F (1 kN)	<0.1% FS
Q_{HP}	Flow meter	Kracht VC12 (600 l/min)	± 0.3%
Q_{Case}	Flow meter	VSE VS1 (80 l/min)	± 0.3%
p_{HP}	Pressure transducer	KELLER PA-23SY (400 bar)	± 0.25% FS
p_{LP}	Pressure transducer	KELLER (30 bar)	± 0.15% FS
p_{Case}	Pressure transducer	HYDAC (16 bar)	± 0.15% FS
T_{HP}	Temperature sensor	HYDAC, -25..+100 °C	± 0.8% FS
T_{LP}	Temperature sensor	HYDAC, -25..+100 °C	± 0.8% FS
T_{Case}	Temperature sensor	HYDAC, -25..+100 °C	± 0.8% FS

To avoid that this run-in interferes with the slipper study, the entire pump was run-in at each OC for a total of over eight hours. Previous studies by the authors have shown that the cylinder block/valve plate gap typically takes up to 30 min to run-in per pressure and speed level [12]. The 8 hours of the standard pump were determined to be sufficient to cover this running-in period. After this running-in period, the flat reference slipper was implemented. To avoid any potential influence from the disassembly, all modifications were carried out by a Parker specialist. Each design was tested multiple times in over 120 OCs, ranging from 500-2300 rpm, 50-350 bar and 25–100 % displacement. These 120 OCs built a Design of Experiment (DOE) set that can be compared to simulation and to each other. In between the measurements of the DOE sets, the pump was also tested to speeds down to 0.1 rpm with (50 and 300 bar) and without pressure to capture low speed and start-up behavior. These ultra-low speed tests were run in between the DOE sets, in order to see if the performance changed after multiple hours at low speed. This process was repeated until no more changes in efficiency were observed between the sets. Then the pump was disassembled, and the next nine slippers (and attached pistons) were replaced. The swash plate was changed only for the step design, as more than expected leakage was observed for the wave design, which could have been due to a worn and therefore not perfectly flat swash plate.

5.2 Full DOE measurement results of the waved slipper at 100% displacement and run-in performance

Although the pump was assumed to be fully run-in, there were still small differences in efficiency at some OCs for each slipper. The variation for the flat reference slipper was small, decreasing by <1% for the 50 bar series, with the largest deviation at 50 bar and 500 rpm being 0.9 percentage points. After disassembly, it was observed that the entire surface of the slipper showed minor wear in the <2µm roughness range. A more detailed analysis of the surface wear can be found in the authors' second paper at this conference.

The waved slipper experienced more pronounced wear. A total of 4 full DOE-sets were measured and are shown in Figure 5.2. The graph shows the total efficiency over speeds from 500-2300 rpm and pressures from 50 to 350 bar, all at 100% displacement. Differently dashed lines indicate different measurement durations ranging from the first measurement after 8 hours to the last measurement after 35 hours. In the low to medium pressure ranges, there were virtually no changes in efficiency. Only at high pressures, increased leakage led to a drop in efficiency. In particular, at low speed and high pressure, changes in the order of 4-5 percentage points were observed in the overall efficiency between the first and last measurement. In contrast to the flat reference design, the changes were in a positive direction, i.e. the overall efficiency increased over time.

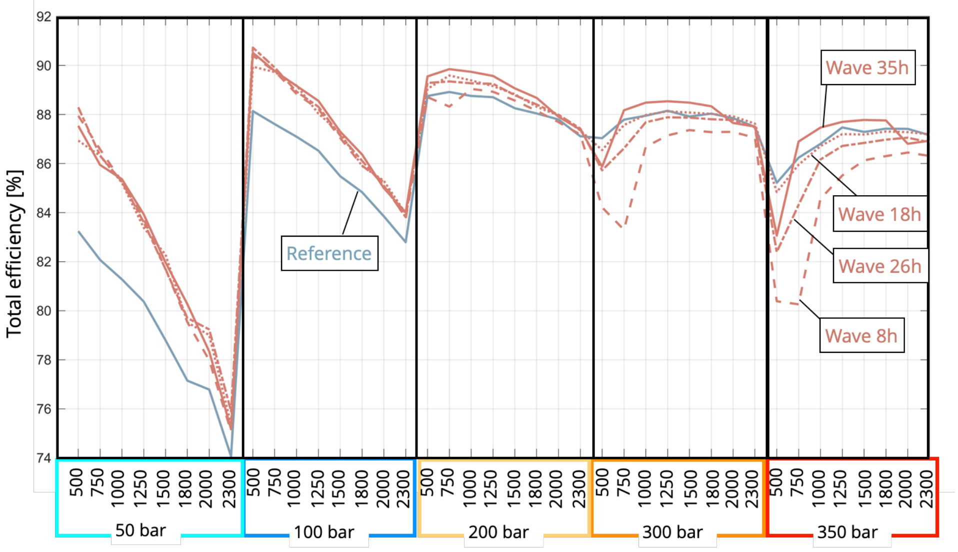

Figure 5.2. Total efficiency for multiple DOE sets of the waved slipper at 100% displacement after different test hours

Unfortunately, after disassembly, the slipper was more worn than expected. Simulation only indicated minor wear at the edges, but not to the extend presented in the surface topology measurements in Figure 5.3. The plot shows 5 µm total wear at the inner edge of the slipper. However, on a positive note, the 6 µm wave was not completely worn off after the tests and the increasing efficiency suggests that the structure will not wear off further. As the valleys (e.g. the lowest part of the wave) were not worn (also indicated by the color in the photos), it was possible to measure the total material loss. This is not possible for the flat slipper as the entire surface has experienced some form of wear. Because of the unaffected valleys, another interesting finding can be observed by the shape of the valleys of the wave. When new, they were perfectly level. After the 35 hours of use, the valleys were shifted by a total of 1.5 µm as indicated by the dotted line in Figure 5.3. This observation can only be explained by a plastic deformation. At the time, it was not known that slippers undergo this type of plastic deformation, so it was never included in any of the simulation models and could have been the cause of the higher than expected wear. Based on the results, it is possible to further improve the wave design and possibly reduce the wear even further.

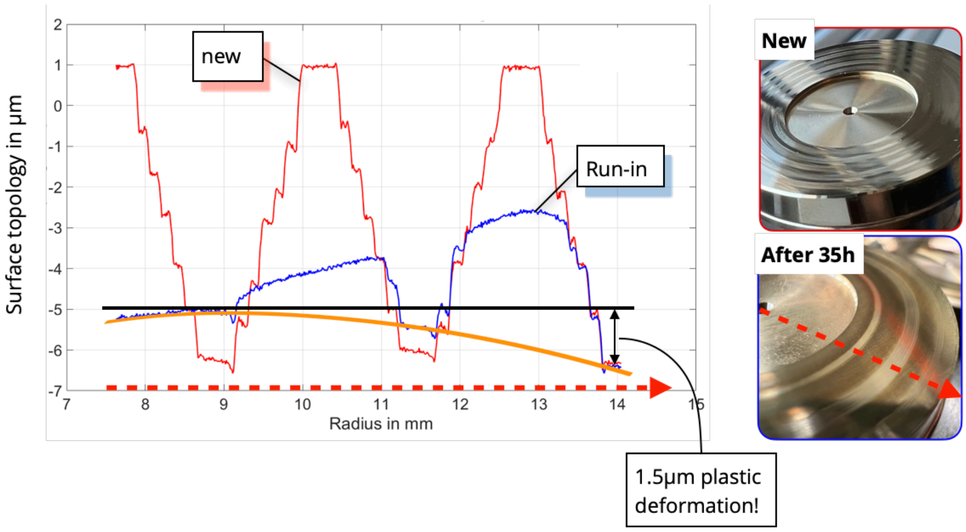

Figure 5.3. Surface topology and photos of the waved slipper new and run-in

5.3 Full DOE measurement results of the step slipper at mutliple displacements in comparison to the reference slipper

The total efficiency map for both the reference and the step slipper for three displacement levels are shown in Figure 5.4. The y-axis represents the pressure level and the shared x-axis the pump speed. Each displacement level has its corresponding color legend. For 100% displacement (top two figures) it is clearly visible, that the step design increases the efficiency predominantly in the lower left corner (low pressure and low speed), while also increasing the dark green area ($\eta_{tot} \geq 90\%$) to medium pressures and speeds.

The efficient area at high speed and low pressure also improved slightly, however this area can usually be improved with the valve plate / cylinder block interface, as this is its most critical OC. The step design greatly improves the efficiencies at low displacements. At 50% displacement (middle figures) the efficiencies below 75% completely disappeared with the step design, while most of the operating conditions now experience efficiencies well above 80%. The drastic rise in efficiency is even more noticeable at 25% displacement (lower figures). Here the reference slipper had no OC with a total efficiency above 70%. After implementing the step slipper the pump now is able to perform at close to 80% total efficiency at low to medium speed and pressures.

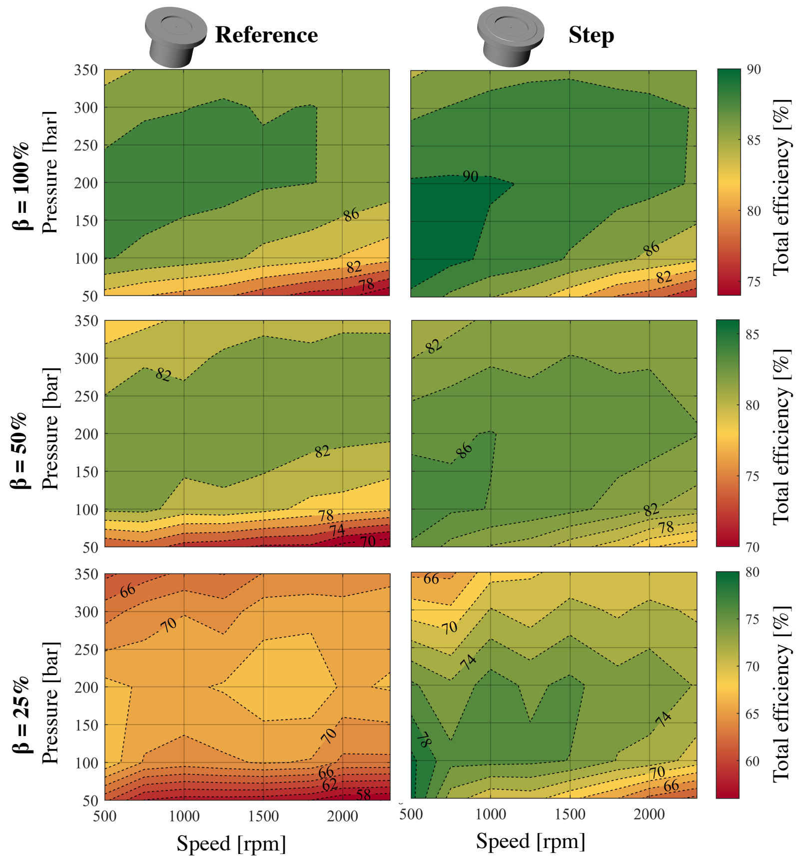

Figure 5.4. Total efficiency characteristic maps of the step design in comparison to the reference for three different swashplate angles

The step design had virtually no run-in. Even after 46 hours of rigorous pump testing the 6µm step had only 1.5 µm of wear on the inner diameter, again due to reduction in surface roughness. A 565 hours endurance test was completed for all designs just prior to publication visual inspection shows that both structures, the wave and the step, are still intact. A more detailed analysis of the run-in of the step-slipper and the manufacturing process is presented in the second paper at this conference by the same authors.

5.4 Efficiency improvements of the structured designs in comparison to the flat reference

Figure 5.5 shows the total efficiency at 100% displacement for the entire operating range for the three tested slipper designs: flat, wave and step. When comparing the waved slipper with the flat reference slipper it can be concluded that the waved slipper has much better low pressure and low speed performance, with an increase of up to 5 percentage points. At low speeds and high pressures the performance of the waved slipped did not increase compared to the flat reference design. At 500 rpm and 350 bar the reference has an advantage of up to 2 percentage points.

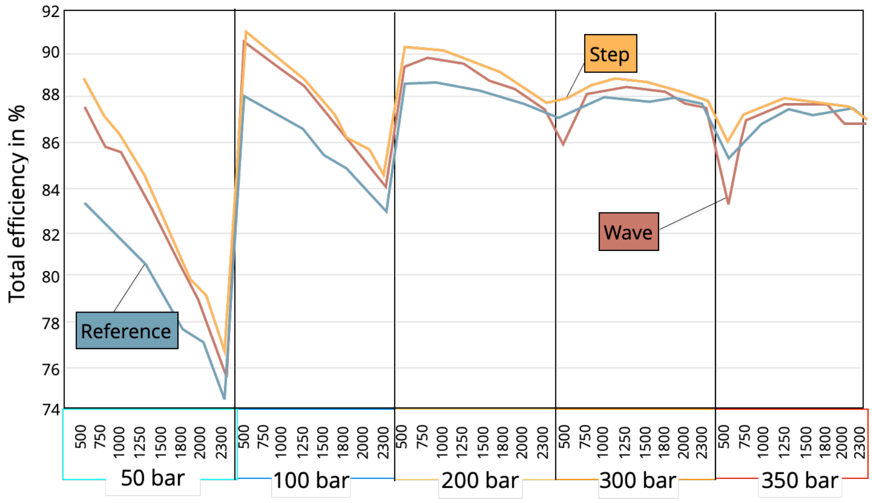

Figure 5.5. Total efficiency of the three different slipper designs at 100% displacement

The slipper with the 6 µm step had the best performance across all operating conditions topping even that of the wave slipper at low pressures and low speeds, while still outperforming the flat reference design at high pressures and high speeds.

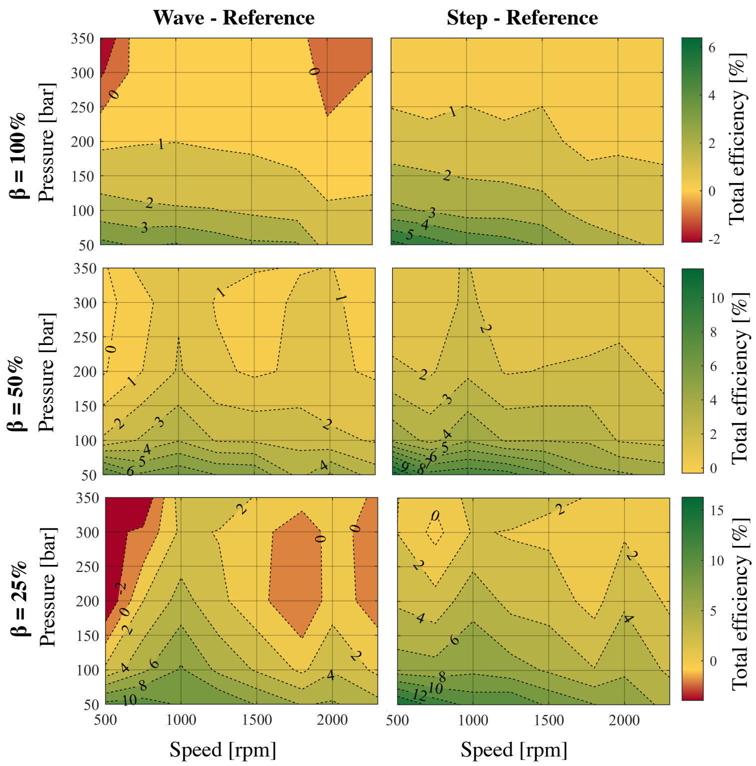

Figure 5.6. Total efficiency differences of the structured designs subtracting the reference at 100%, 50% and 25% displacement

For lower swash plate angles the efficiency gain was even more drastic as can be seen in the change in the efficiency maps shown in Figure 5.6. Here the difference between the total efficiency between the wave and reference slipper (left) and step and reference slipper (right) is shown. The higher the values the more total efficiency point gain was achieved by the design. While the waved slipper achieved great results at low pressure, it also led to up to 2 percentage point losses at 100% and high pressure. The step design had no OC where it had a noticeable efficiency drop compared to the reference design. The overall efficiency point increase from the step design compared to the flat design is 6 percentage points at 100%, 11 percentage points at 50% displacement and up to 16 percentage points at 25% displacement, all at 500 rpm and 50 bar.

5.5 *Performance at extremely low speeds*

Both the wave and the step slipper had an exceptionally good low and ultra-low speed performance. Figure 5.7 shows the measured torque loss at 50 bar for all three slipper designs (left) and the correspoding leakage losses (right). An additional measurement of the step slipper in lead-free material with a lead content of <0.1% has been carried out. The speed is shown on a logarithmic scale to highlight the ultra-low speed torque. The wave slipped and the step slipper outperform the reference slipper across the entire speed range for 50 bar. Both the wave and step design have a similar low torque loss, reducing the torque loss up to 80%. To recollect, the shown torque loss reflects the losses for the entire pump, which highlights how much influence the slipper has for low speed performance in axial piston pumps.

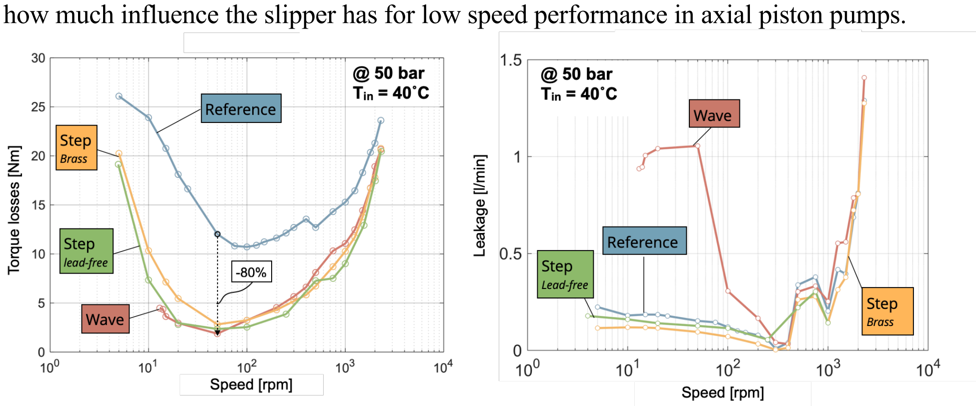

Figure 5.7. Torque loss (left) and leakage (right) at 50 bar for the different designs

The brass and lead-free step slipper have an even lower leakage than the reference, even though having a larger pocket size. This can be explained by overall lower gap heights and a reduction in tilt. The wave design however has a much higher leakage at low rpm (<200 rpm). This was not predicted by the simulation and will be further investigated.

The torque loss at 300 bar is shown in Figure 5.8 left with the corresponding leakage losses in the right. At 300 bar the step design outperforms the flat design starting at 100 rpm with a maximum torque reduction of 16%. However, below 100 rpm the two slipper designs have a very similar torque curve. In contrast to that, the wave slipper design exhibits an essentially flat torque curve from 30 to 500 rpm, leading to a 60 % reduction of torque at 30 rpm. It is not clear, why the lead-free step slipper has such a different torque and leakage curve compared to the brass step slipper. It could be due to the short operating time of only 10 hours.

The leakage results are similar to the trends of the 50 bar measurements. The wave slipper leaks 2 l/min at 30 rpm, whereas the reference pump produces 1 l/min leakage. For more low speed analysis including cold start-up and wear measurements refer to the second paper of the authors in this conference.

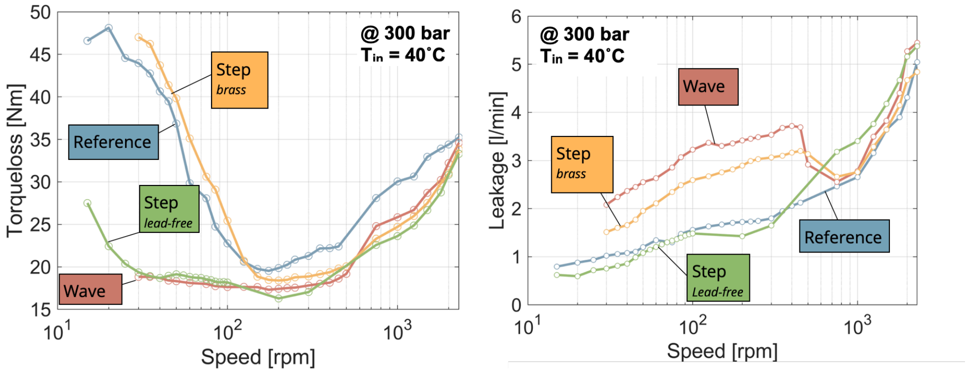

Figure 5.8. Torque loss (left) and leakage (right) at 300 bar for the different designs

6 COMPARISON TO SIMULATION RESULTS

The comparison between the designs is only possible in relation to each other, as the entire pump is measured instead of just the slippers. A similar problem is faced with comparing the simulation with measurement. In order to compare the 4 OC the wave and step design power losses were subtracted from flat design. This was done for both the simulation and measurement and compared in Figure 6.1. The two columns are the wave slipper (left) and the step slipper (right). In each column there are simulation results (compare to Figure 4.2) and measurement results. The waved design was predicted to have a 12% increase in efficiency at OC1 in comparison to the reference slipper. Similarly, the simulation predicted a slightly lower increase at OC3 while having a small efficiency reduction at OC2 and virtually unchanged at OC4. In measurement the trend is the same, but with more improvement at OC3 but also worse at OC2. The waved slipper has virtually no effect on OC4 both in simulation and measurement

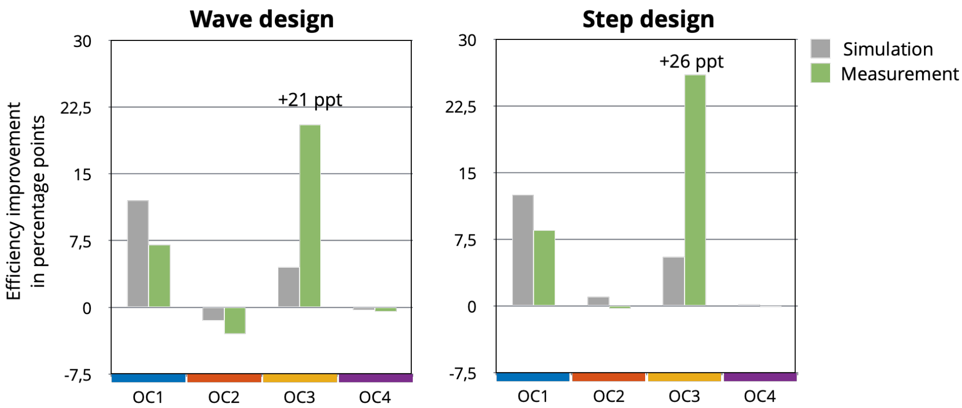

Figure 6.1. Comparison between simulation and measurement

For the step design the simulation expected a large increase in efficiency at OC1 and OC3 and a small to no increase for OC2 and OC4. The measurement confirms the simulated trend. However, OC3 highly outperforms expectations and OC1 has slightly less improvements. OC3 has small reduction in efficiency instead of an increase and OC4 is essentially unchanged as predicted. Overall there is a very good match between the simulation results and the measurement, further increasing the confidence in using numerical simulation tools such as Caspar FSTI as the only necessary design tool, and using measurements only as confirmation rather than a step in the design chain.

7 Summary and Conclusion

Surface structures have a potential to increase hydrostatic machines performance. This was shown in the past for example for the valve plate by Baker [7]. This paper presents the measurement results of two viable surface structures of the slipper. A wave like structure, leaning on the results from Baker has shown to be able to reduce the friction at low pressure and high pressure across the entire operating range. However, the powerlosses increased due to leakage at high pressure and the design showed wear and plastic deformation, leaving room for improvement if such a structure should be used for future pump types. The torque loss at 300 bar is very impressive, staying nearly constant from 30 to 500 rpm. The plastic deformation could be incorporated in the future simulation results further improving this design.

A new step-like structure has shown tremendous potential for slipper and, by extension, other hydrostatic bearings. This 6 µm step has not only reduced the start-up torque by more than half, but has also improved performance in almost all operating conditions, particularly under partial load conditions such as low speed, low pressure or low displacement. This design has virtually no wear, with only 1.5 µm on the inner surface, after rigorous testing over the entire operating range. This was confirmed by a 565 hour accelerated lifetime test, where the slipper showed similar wear to the tests after 35 hours. It is also very easy to manufacture, at least compared to the wave-type structure. These results open up new possibilities for pumps at low speeds and especially lead-free designs, as this slipper essentially does not have to withstand metal to metal contact. Such a lead-free slipper has been successfully tested with the step design and the results are presented in the second paper at this conference from the same author, entitled “Design of a Lead-Free Slipper Bearing for Low Speed Axial Piston Pump Applications”. In the future, all lubrication gaps could benefit from such structures, further increasing efficiency and allowing virtually any speed operation in combination with electric drives.

8 Acknowledgment

The presented research activities are part of the project “Tribologieoptimierung von Pumpensystemen durch fertigungsgerechte Einbringung von Mesostrukturen” (Ref. No. 20757 BR/1). The authors would like to thank the Fluid Power Research Fund of the VDMA for the funding and support.

9 References

[1] B. Kim, Y. H. Chae, and H. S. Choi, “Effects of surface texturing on the frictional

behavior of cast iron surfaces," *Tribol. Int.*, vol. 70, pp. 128–135, 2014.

[2] H. Murrenhoff and A. Hoppermann, "Verbessertes Verschleiß- und Reibgungsverhalten hydraulischer Komponenten durch laserstrukturierte Kontaktflächen," 2004.

[3] M. VDMA, "Abschlussbericht Mathematische Modellierung , Optimierung und Herstellung mikrostrukturierter Kontaktflächen für hydraulische Verdrängereinheiten - OptiKonS," 2010.

[4] J. Baker and M. Ivantysynova, "Advanced Surface Design for Reducing Power Losses in Axial Piston Machines," *11th Scand. Int. Conf. Fluid Power, SICFP*, 2009.

[5] M. Ivantysynova and R. Lasaar, "An investigation into micro- and macrogeometric design of piston/cylinder assembly of swash plate machines," *Int. J. Fluid Power*, vol. 5, no. 1, pp. 23–36, 2004.

[6] M. Ernst, A. Vacca, M. Ivantysynova, and G. Enevoldsen, "Tailoring the Bore Surfaces of Water Hydraulic Axial Piston Machines to Piston Tilt and Deformation," pp. 1–29, 2020.

[7] A. M. Wondergem and M. Ivantysynova, "The Impact of the Surface Shape of the on Power Losses," in *FPNI*, 2014, pp. 1–12.

[8] J. Ivantysyn, "Sliding bearing with self-adjusted load bearing capacity," US5983781A, 1997.

[9] N. R. Kane, J. Sihler, and A. H. Slocum, "A hydrostatic rotary bearing with angled surface self-compensation.," *Precis. Eng. 27.2*, pp. 125–139, 2003.

[10] S. Horn, R. Ivantysyn, and J. Weber, "Tribo-optimized lubricating interfaces in hydrostatic pumps with surface shaped slippers," 2022.

[11] J. Ivantysyn and M. Ivantysynova, *Hydrostatic Pumps and Motors*. Academic Books International, 2001.

[12] R. Ivantysyn, A. Shorbagy, and P. J. Weber, "Analysis of the Run-in Behavior of Axial Piston Pumps," in *IEEE GFPS 2018*, 2018.

Biographies

Svenja Horn received her diploma degree in aircraft construction from Technical University of Dresden in 2018. Since 2018 she is working as a research assistant at the Chair of Fluid-Mechatronic Systems on the efficiency and lifetime improvement and optimization of axial piston pumps. Her research focus on the tribological phenomena of the slipper/swashplate interface as well as the implementation of machine learning algorithms to monitor the pump’s service life. Her PhD thesis deals with increasing efficiency through meso-structured surfaces and examines the physical effects and functioning of structuring in more detail

Roman Ivantysyn received his bachelor's and master’s degrees in mechanical engineering from Purdue University in 2008 and 2011, respectively. Since 2011, he has been working as a research assistant at the Chair of Fluid-Mechatronic Systems (Fluidtronics) at the Technical University of Dresden, focusing on systems and components. His research topics include open circuit displacement control in mining excavators, pump design and thermal gap analysis in axial piston pumps. He is set to submit his PhD thesis, titled “Thermal Investigation of the Lubricating Gaps of an Axial Piston Pump with Respect to Efficiency and Wear,” this year.